International Journal For Advanced Research In Science & Technology
A peer reviewed international journal www.ijarst.in
ISSN: 2457-0362

Solar PV-Powered SRM for EV system with Fuzzy Logic Controller

LOTHA ESWARA KUMAR
M.Tech Student Scholar
Department of Electrical & Electronics Engineering
BABA Institute of Technology & Sciences
P.M.Palem, Visakhapatnam (Dt), A.P, India.
E-Mail: eswarlotha225@gmail.com

K.VENKATESWARA RAO
Assistant Professor
Department of Electrical & Electronics Engineering
BABA Institute of Technology & Sciences
P.M.Palem, Visakhapatnam (Dt), A.P, India.
E-Mail: kasivenki206@gmail.com

Abstract:
This study describes the use of fuzzy logic control (FLC) to the speed control of a switching reluctance motor (SRM). Because of its advantages over traditional AC/DC drives, Switched Reluctance Motors (SRM) have a wide range of industrial applications. This is owing to the simple structure, toughness and low-cost production possibilities. SRM speed has been controlled using a variety of approaches. In principle, the PV-fed EV is similar to the hybrid electric vehicle in that the internal combustion engine (ICE) is replaced with a PV panel. PV has distinct properties than ICEs; maximum power point tracking (MPPT) and solar energy usage are the distinguishing features of PV-fed EVs. In order to achieve low cost and variable energy flow modes, this article proposes a low cost tri-port converter to coordinate the PV panel, SRM, and battery. The FLC employs a PI-like control technique, providing the current reference variation based on speed error and its variation. The drive system's performance was assessed using the MATLAB/SIMULINK software.

Keywords: Electric vehicles, photovoltaic's (PV), power flow control, switched reluctance motors (SRMs), tri-port converter, Fuzzy Logic Controller.

I. INTRODUCTION

Photovoltaic Generators (PV) are a renewable and limitless source of electricity. As part of an ongoing study on low-cost PV-powered Electrical Vehicles, a control system for a specific configuration is examined here, based on PV panels that power a Switched Reluctance Motor, with independent controllers for maximizing power supply and optimizing motor operation [1-3]. In this study, the Simulink model for speed control of a switching reluctance motor is implemented utilizing several speed controllers [4]. The simulink models are created individually for the P, PI, and Fuzzy logic controllers, and their performance results are compared [5]. The Switched Reluctance Motor is a type of electric motor that operates on reluctance torque. For industrial applications, a motor with a speed of 50,000 rpm is employed [6]. The speed controllers used in this study are based on traditional P& PI controllers, while the other is an AI-based Fuzzy Logic Controller [7].

The PI Controller (proportional integral controller) is a subset of the PID controller that does not employ the error derivative [8]. A fuzzy logic controller is a highly intelligent controller that processes input using fuzzy logic [9]. Fuzzy logic is a multi valued logic that is similar to human reasoning [10]. FLC offers a variety of applications in industrial control, particularly where traditional control design approaches are challenging to apply [11]. SRM machine modeling, design, simulation, analysis, and control have all been thoroughly reviewed.

The control system seeks to manage the PV generators so that they are constantly at the Maximum PowerPoint (MPP) (which varies with the levels of solar radiation and panel temperature, as well as the characteristics of the load linked to the PV) [12]. As a result, in order to collect the most possible power from the panel, a Maximum Power Point Tracking (MPPT) method is adopted [13]. Many approaches for determining Maximum Power Point Tracking (MPPT) have been developed: The difficulty of linking different energy sources to power an electrical motor in an off-grid situation is addressed in this work [14]. When a PV generator supplies an SRM load via a SEPIC converter, the duty cycle is regulated by a particular MPPT controller [15]. The duty cycle of the converter is estimated and changed in this research to optimize the power functioning of the entire system.

In general, the PV-fed EV has a similar construction to the hybrid electric vehicle, with the PV panel replacing the internal combustion engine (ICE). Figure 1 depicts the PV-fed EV setup. Its main components are an off-board charging station, a photovoltaic (PV), batteries, and power converters. One

International Journal For Advanced Research In Science & Technology
A peer reviewed international journal
www.ijarst.in
ISSN: 2457-0362

option to reducing energy conversion procedures is to reconfigure the motor to include certain on-board charging operations. Paper, for example, builds a 20-kW split-phase PM motor for EV charging, but it has significant harmonic contents in the reverse electromotive force (EMF). Another option is to use a standard SRM. Paper uses machine windings as the input filter inductor to enable on-board charging and power factor correction in a 2.3-kW SRM. The notion of driving topology modular structure is given in this study. A four-phase half bridge converter based on intelligent power modules (IPM) is used to achieve driving and grid-charging. Although modularization facilitates mass manufacturing, using a half/full bridge architecture affects system dependability (e.g. shoot-through issues). The paper proposes a basic architecture for a plug-in hybrid electric vehicle (HEV) that allows for variable energy flow. However, in order to charge the grid, the grid must be linked to the generator rectifier, which increases the energy conversion process and affects charging efficiency. Nonetheless, a viable architecture and control method for PV-powered EVs has yet to be devised. Because PV differs from ICEs in many ways, the maximum power point tracking (MPPT) and solar energy consumption are distinguishing features of PV-fed EVs.

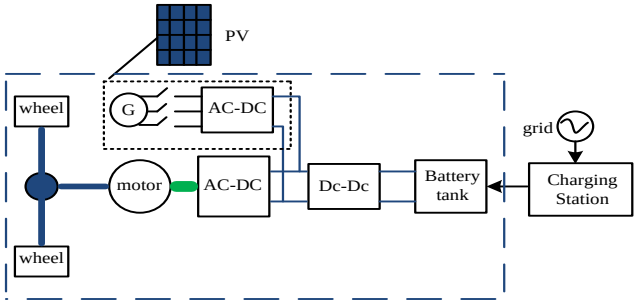

Fig.1 PV-fed hybrid electrical vehicle

II. TOPOLOGY AND OPERATIONAL MODES

A. Proposed topology and working modes

Three energy terminals are suggested in the proposed Tri-port topology: PV, battery, and SRM. As illustrated in Fig.2 [26], they are coupled by a power converter composed of four switching devices (S0S3), four diodes (D0D3), and two relays. The six operating modes are provided by controlling relays J1 and J2, as indicated in Fig. 3; the associated relay actions are listed in Table I. PV is the energy source used to power the SRM and charge the battery in mode 1. In mode 2, the PV and battery are both used to power the SRM. In mode 3, the PV serves as the source, while the battery sits idle. In mode 4, the battery serves as the power source, and the PV is turned off. In mode 5, the battery is charged by a single-phase grid while the PV and SRM are turned off. In mode 6, the PV charges the battery while the SRM is idle.

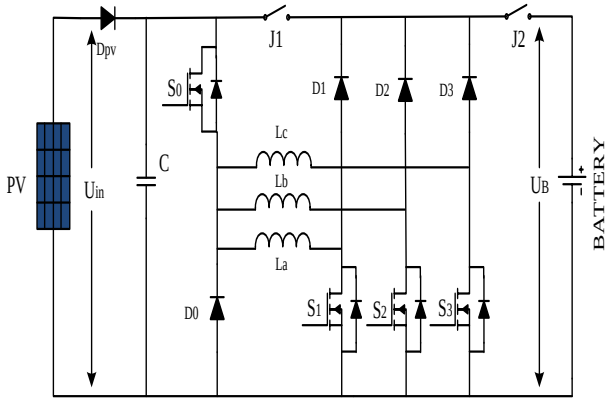

Fig.2. The proposed Tri-port topology for PV-powered SRM drive

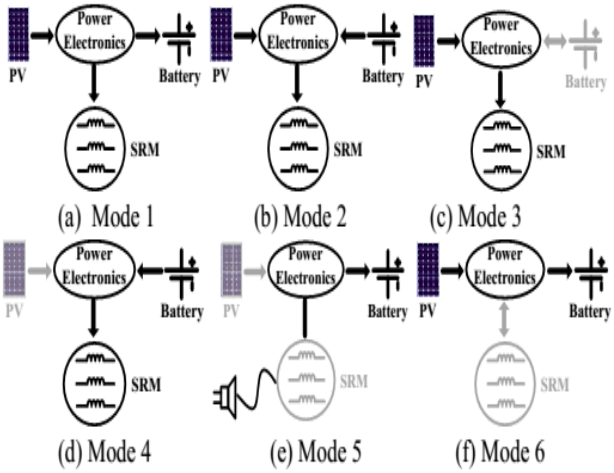

Fig.3. Six operation modes of the proposed Tri-port topology

TABLE 1 J1 and J2 Actions under Different Modes

Mode	J1 and J2
1	J1 turn off : J2 turn on
2	J1 and J2 turn on
3	J1 turn on: J2 turn off
4	J1 and J2 turn on
5	J1 and J2 turn on
6	J1 turn off: J2 turn on

International Journal For Advanced Research In Science & Technology
A peer reviewed international journal
www.ijarst.in
ISSN: 2457-0362

B. Driving modes

Operating modes 1~4 are the driving modes to provide traction drive to the vehicle.

(1) Mode 1

At light loads, the energy provided by the PV is greater than the SRM required; the system functions in mode 1. Figure 4 (a) depicts the analogous operating circuit, in which relay J1 is turned off and relay J2 is turned on. The energy from the PV panels is sent into the SRM, which charges the battery; hence, in this mode, the battery is charged in the EV operation condition.

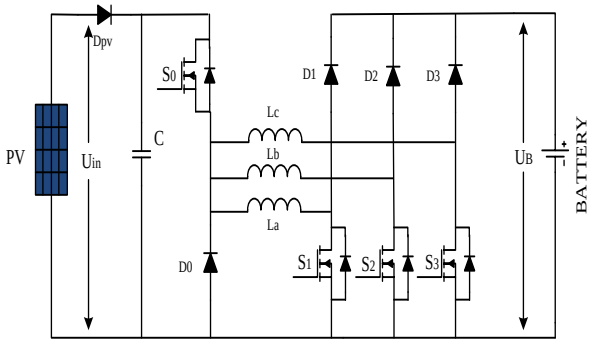

(a) Operation circuit under mode 1

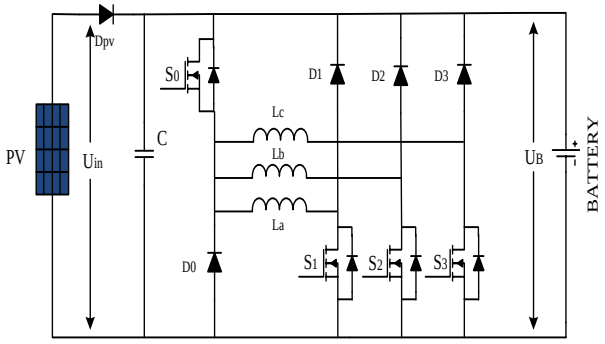

(b) Operation circuit under mode 2

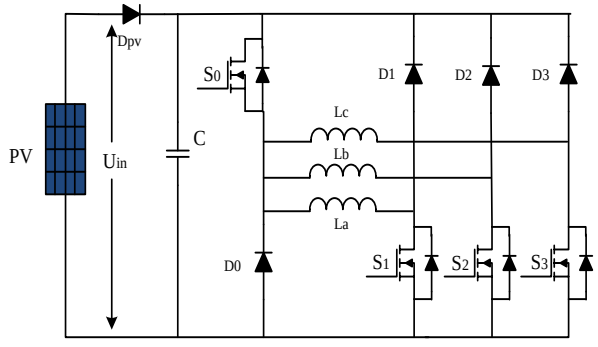

(c) Operation circuit under mode 3

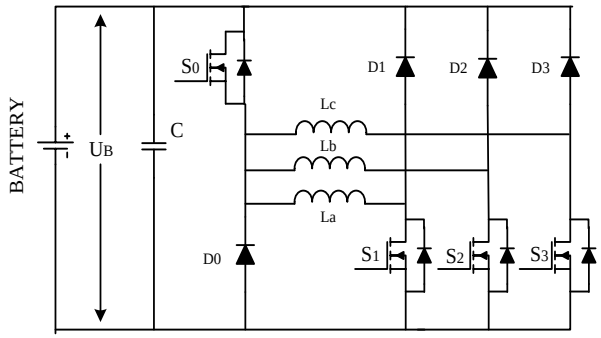

(d) Operation circuit under mode 4

Fig.4 The equivalent circuits under driving modes

(2) Mode 2

While the SRM is under significant load, such as when going uphill or accelerating, both the PV panel and the battery deliver electricity to the SRM. Figure 4(b) depicts the analogous operating circuit, in which relays J1 and J2 are switched on.

(3) Mode 3

When the battery runs out of electricity, the PV panel is the only source of energy to operate the car. Figure 4 depicts the comparable circuit (c). J1 is turned on, and J2 is turned off.

(4) Mode 4

When the PV cannot generate electricity owing to insufficient solar irradiation, the SRM is powered by the battery. Figure 4 depicts the equivalent topology (d). Relay J1 and J2 are both conducting in this mode.

C. Battery charging modes

Operating modes 5 and 6 are the battery charging modes.

(5) Mode 5

When PV is unable to generate energy, an additional power source, such as the AC grid, is required to charge the battery. Figure 5 depicts the comparable circuit (a). J1 and J2 are turned on. Point A is the centre tapped phase winding, which is readily accomplished without modifying the motor assembly. As indicated in Fig.5, one of the three phase windings is divided and its midway is taken out (a). As input filter inductors, phase windings La1 and La2 are used. These inductors are used as part of the driving circuit to create an AC-DC rectifier for grid charging.

(6) Mode 6

The PV can charge the battery when the EV is parked in the sun. J1 is turned off, while J2 is turned on. Figure 5 depicts the relevant charging circuit (b).

International Journal For Advanced Research In Science & Technology
A peer reviewed international journal
www.ijarst.in
ISSN: 2457-0362

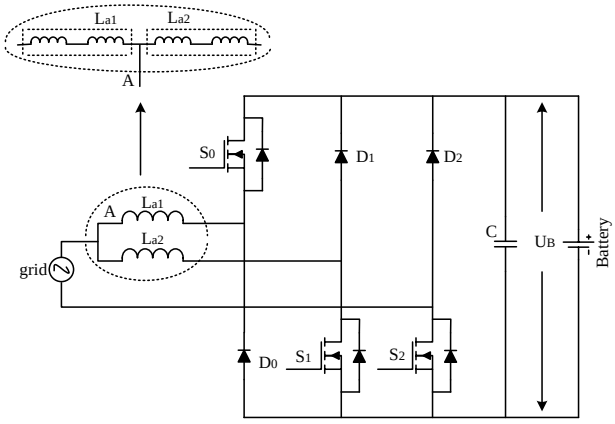

(a) Grid charging mode

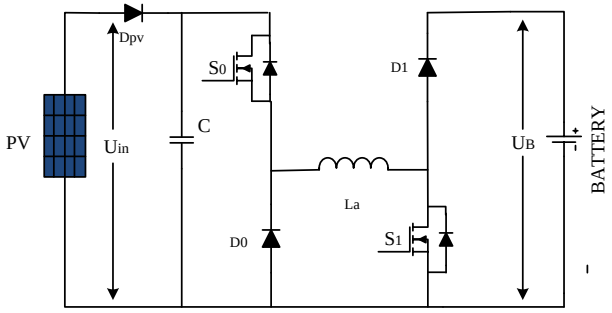

(b) PV source charging mode

Fig.5 Equivalent circuits of charging condition modes

III. Control Strategy under Different Modes

A control approach with several modes is developed to make the best use of solar energy for driving the EV.

B. Single source driving mode

There are three types of power sources: PV-driving, battery-driving, and PV plus battery parallel feeding sources. When the PV power cannot support the EV under heavy load, mode 2 can be used to provide adequate energy and make full use of solar energy. The equivalent power source is depicted in Fig.6(a), and the corresponding PV panel operating points are depicted in Fig.6(b). The PV panel voltage is constrained to the battery voltage UB since it is paralleled with the battery. As illustrated in Fig.7, there are three operating stages in mode 2: winding excitation, energy recycling, and freewheeling. Modes 3 and 4 feature operational states that are comparable to mode 2. The difference is that in mode 3, the PV is the sole source, and in mode 4, the battery is the only source.

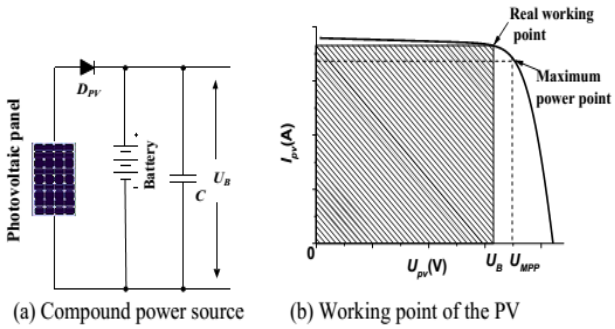

(a) Compound power source (b) Working point of the PV

Fig.6 Power supply at mode 2

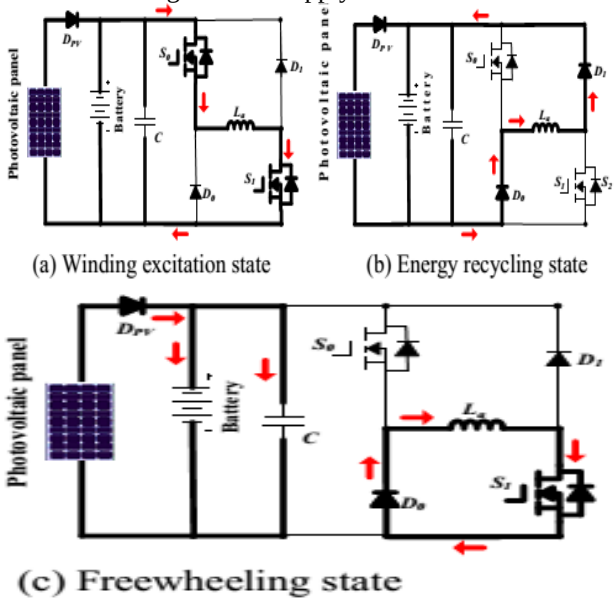

(a) Winding excitation state (b) Energy recycling state

(c) Freewheeling state

Fig.7 Working states at mode 2

Neglecting the voltage drop across the power switches and diodes, the phase voltage is given by

$$U_{in} = R_k I_k + \frac{d\varphi(i_k,\theta_r)}{dt}$$

$$= R_k I_k + L_k \frac{di_k}{dt} + i_k \omega_r \frac{dL_k}{d\theta_r}\ ,\ k = a,b.c \qquad (1)$$

where U_{in} is the DC-link voltage, k is phase a, b, or c, R_k is the phase resistance, i_k is the phase current, L_k is the phase inductance, θr is the rotor position, $\psi(i_k, \theta_r)$ is the phase flux linkage depending on the phase current and rotor position, and ωr is the angular speed. The third term in Eq.1 is the back electromotive force (EMF) voltage given by

$$e_k = i_k \omega_r \frac{dL_k}{d\theta_r} \qquad (2)$$

Hence, the phase voltage is found by

$$U_k = R_k i_k + L_k \frac{di_k}{dt} + e_k \qquad (3)$$

In the excitation region, turning on S0 and S1 will induce a current in phase a winding, as show in

International Journal For Advanced Research In Science & Technology
A peer reviewed international journal
www.ijarst.in
ISSN: 2457-0362

Fig.7(a). Phase a winding is subjected to the positive DC bus voltage.

$$+U_{in} = R_k i_k + L_k \frac{di_k}{dt} + e_k \quad (4)$$

When S0 is off and S1 is on, the phase current is in a freewheeling state in a zero voltage loop, as shown in Fig.3.7(c), the phase voltage is zero.

$$0 = R_k i_k + L_k \frac{di_k}{dt} + e_k \quad (5)$$

In the demagnetization region, S0 and S1 are both turned off, and the phase current will flow back to the power supply, as show in Fig.7(b). In this state, the phase winding is subjected to the negative DC bus voltage, and the phase voltage is

$$-U_{in} = R_k i_k + L_k \frac{di_k}{dt} + e_k \quad (6)$$

In single source driving mode, the voltage-PWM control is employed as the basic scheme, as illustrated in Fig.8. According to the given speed ω*, the voltage-PWM control is activated at speed control.

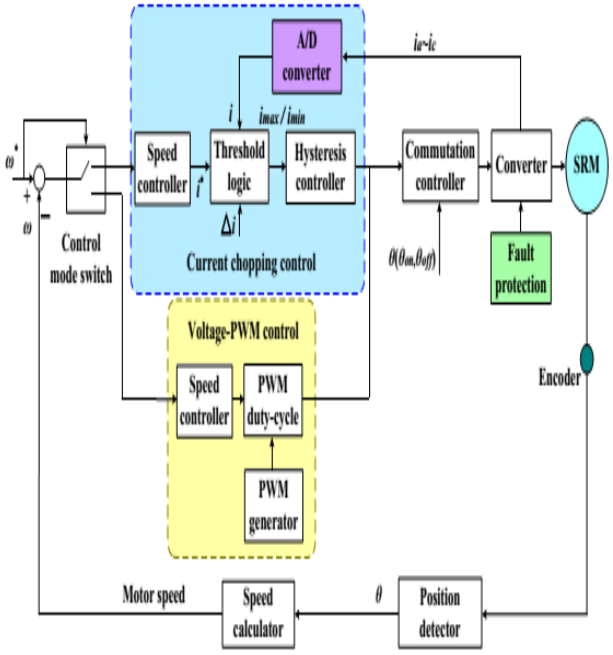

Fig.8 SRM control strategy under single source driving mode

B. Driving-charging hybrid control strategy

The PV is the driving source in the driving-charging hybrid control, and the battery is charged by the freewheeling current, as shown in drive mode 1. There are two control goals: maximum power point tracking (MPPT) of the PV panel and SRM speed control.

The dual-source condition is changed from a PV-driving mode to a non-PV-driving mode. In mode 3, the motor speed is first controlled at a preset pace. Then, to switch to mode 1, J2 is turned on and J1 is turned off. The maximum power of a PV panel may be tracked by changing the turn-off angle.

The dual-source mode (mode 1) has three stable operating states, as shown in Fig.9. In Fig.9(a), S0 and S1 conduct, and the PV panel charges the SRM winding to drive the motor. In Fig.9(b), S0 and S1 switch off, and the battery is charged with the phase winding's freewheeling current. Figure 9(c) depicts a freewheeling condition.

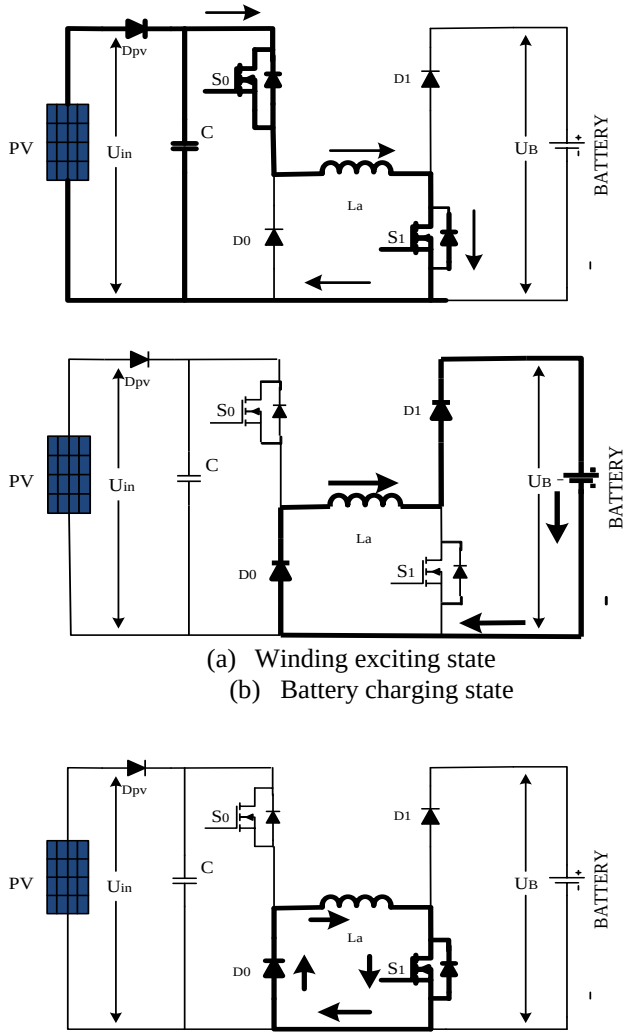

(a) Winding exciting state
(b) Battery charging state
(c) Freewheeling state

Fig.9 Mode 1 working states

Fig.10 is the control strategy under driving-charging mode. In Fig.10, θon is the turn on angle of SRM; θoff is the turn-off angle of SRM. By adjusting turn-on angle, the speed of SRM can be controlled; the maximum power point tracking of PV panel can be achieved by adjusting turn-off angle, which can control the charging current to the battery.

International Journal For Advanced Research In Science & Technology
A peer reviewed international journal
www.ijarst.in
ISSN: 2457-0362

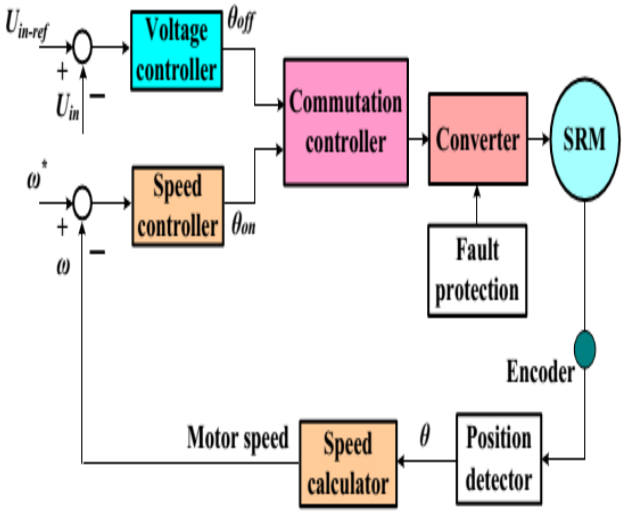

Fig.10. Control strategy under driving-charging mode (mode 1)

C. Grid-charging control strategy

The proposed topology also supports the single-phase grid charging. There are four basic charging states and S0 is always turned off. When the grid instantaneous voltage is over zero, the two working states are presented in Fig.11(a) and (b). In Fig.11(a), S1 and S2 conduct, the grid voltage charges the phase winding La2, the corresponding equation can be expressed as Eq.7; In Fig.11(b), S1 turns off and S2 conducts, the grid is connected in series with phase winding to charges the battery, the corresponding equation can be expressed as Eq.8.

$$U_{grid} = L_{a2}.\frac{di_{grid}}{dt} \tag{7}$$

$$U_B - U_{grid} = L_{a2}.\frac{di_{grid}}{dt} \tag{8}$$

When the grid instantaneous voltage is below zero, the two working states are presented in Fig.11 (c) and (d). In Fig.11(c), S1 and S2 conduct, the grid voltage charges the phase winding La1 and La2, the corresponding equation can be expressed as Eq. (9); In Fig.11(d), S1 keeps conducing and S2 turns off, the grid is connected in series with phase winding La1 and La2 to charges the battery, the corresponding equation can be expressed as Eq.10.

$$U_{grid} = \frac{L_{a1}+L_{a2}}{L_{a1}.L_{a2}}.\frac{di_{grid}}{dt} \tag{9}$$

$$-U_B - U_{grid} = \frac{L_{a1}+L_{a2}}{L_{a1}.L_{a2}}.\frac{di_{grid}}{dt} \tag{10}$$

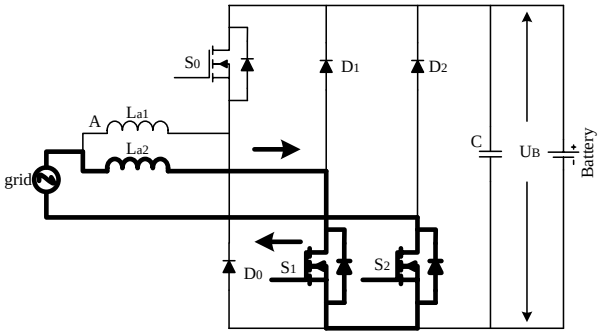

(a) Grid charging state 1 (Ugrid>0)

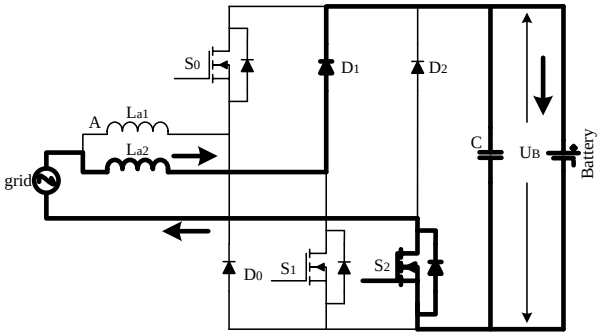

(b) Grid charging state 2 (Ugrid>0)

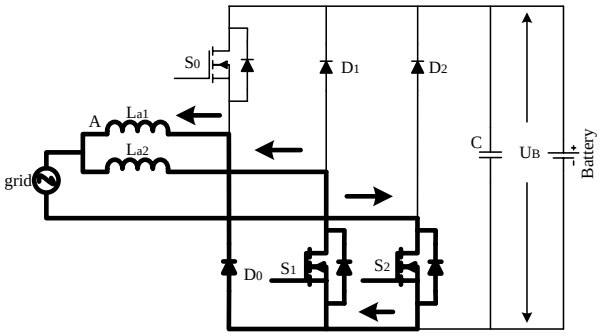

(c) Grid charging state 3 (Ugrid<0)

International Journal For Advanced Research In Science & Technology
A peer reviewed international journal
www.ijarst.in
ISSN: 2457-0362

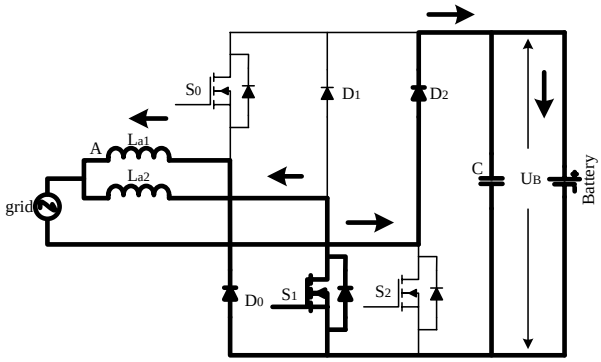

(d) Grid charging state 4 (Ugrid<0)

Fig.3.11 Mode 5 charging states

In Fig.12, Ugrid is the grid voltage; by the phase lock loop (PLL), the phase information can be got; Iref_grid is the given amplitude of the grid current. Combining sinθ and Iref_grid, the instantaneous grid current reference iref_grid can be calculated. In this mode, when Ugrid> 0, the inductance is La2; when Ugrid< 0, the inductance is paralleled La1 and La2; in order to adopt the change in the inductance, hysteresis control is employed to realize grid current regulation. Furthermore, hysteresis control has excellent loop performance, global stability and small phase lag that makes grid connected control stable.

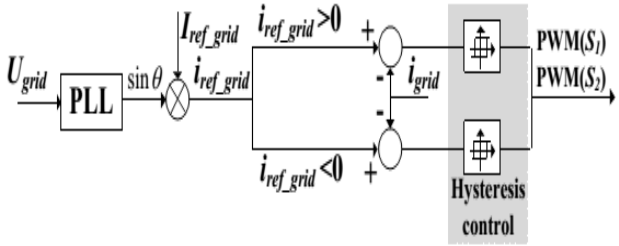

Fig.12 Grid-connected charging control (Mode 5)

D. PV-fed charging control strategy

In this mode, the PV panel charges the battery directly by the driving topology. The phase windings are employed as inductor; and the driving topology can be functioned as interleaved Buck boost charging topology. For one phase, there are two states, as shown in Fig.13(a) and (b). When S0 and S1 turn on, the PV panel charges phase inductance; when S0 and S1 turns off, the phase inductance discharges energy to battery. According to the state-of-charging (SoC), there are three stages to make full use of solar energy and maintain battery healthy condition, as illustrated in Fig.13 (c). During stage 1, the corresponding battery SoC is in 0~SoC1, the battery is in extremely lack energy condition, the MPPT control strategy is employed to make full use of solar energy. During stage 2, the corresponding battery SoC is in SoC1~ SoC2, the constant voltage control is adapted to charging the battery. During stage 3, the corresponding battery SoC is in SoC2~1, the micro current charging is adapted. In order to simplify the control strategy, constant voltage is employed in PV panel MPPT control.

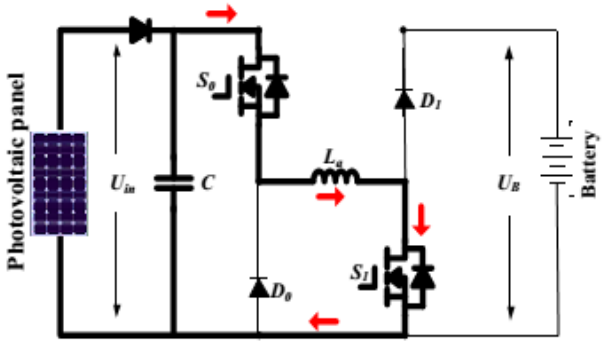

(a) Phase inductance charging

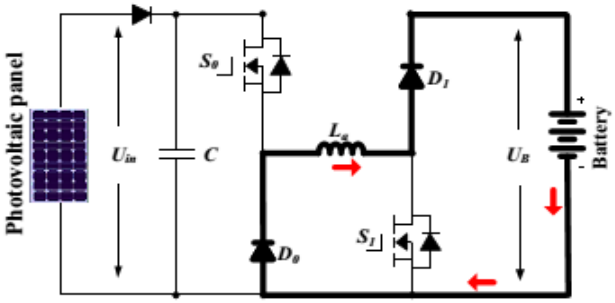

(b) Battery charging

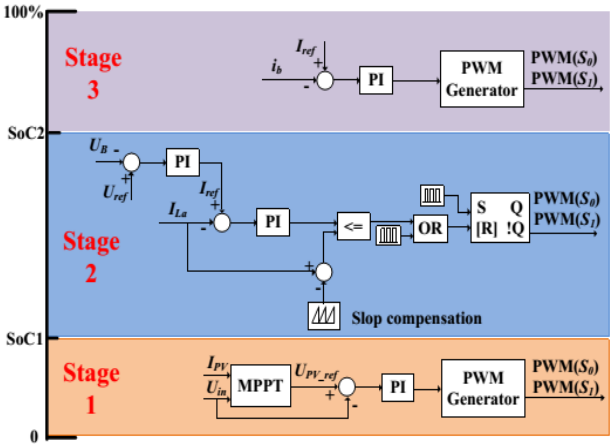

(c) Charging control strategy.

Fig.13 Mode 6 charging states and control strategy.

IV. DESIGN OF A FUZZY CONTROLLER

The difficulty regarding the PI controller gain is the fine tuning of the controller so as to achieve the optimal operation of the task. The major drawback of the PI controller is faced when the process is nonlinear and also when the system is having oscillations. Considering all these facts, a fuzzy logic controller was implemented. A fuzzy controller can work in linear as

International Journal For Advanced Research In Science & Technology
A peer reviewed international journal
www.ijarst.in
ISSN: 2457-0362

well as in nonlinear design parameters. FL requires some numerical parameters in order to operate such as what is considered significant error and significant rate-of-change-of error, but exact values of these numbers are usually not critical unless very responsive performance is required in which case empirical tuning would determine them.

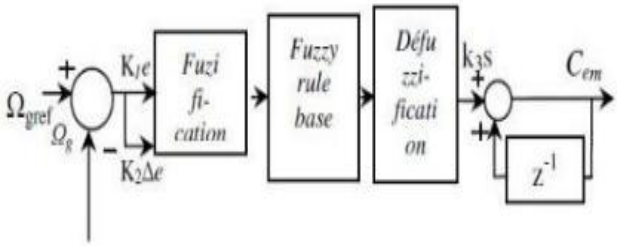

Fig.14 Fuzzy Logic Controller

FL requires some numerical parameters in order to operate such as what is considered significant error and significant rate-of-change-of-error, but exact values of these numbers are usually not critical unless very responsive performance is required in which case empirical tuning would determine them. For example, a simple temperature control system could use a single temperature feedback sensor whose data is subtracted from the command signal to compute "error" and then time-differentiated to yield the error slope or rate of change-of-error, hereafter called "error-dot".

V. MATLAB/SIMULATION RESULTS

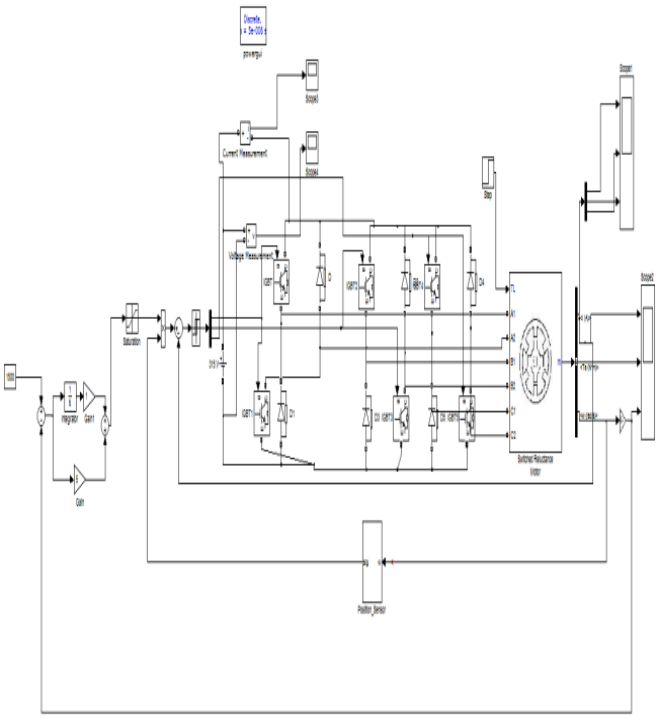

Fig.15 SRM drive model diagram

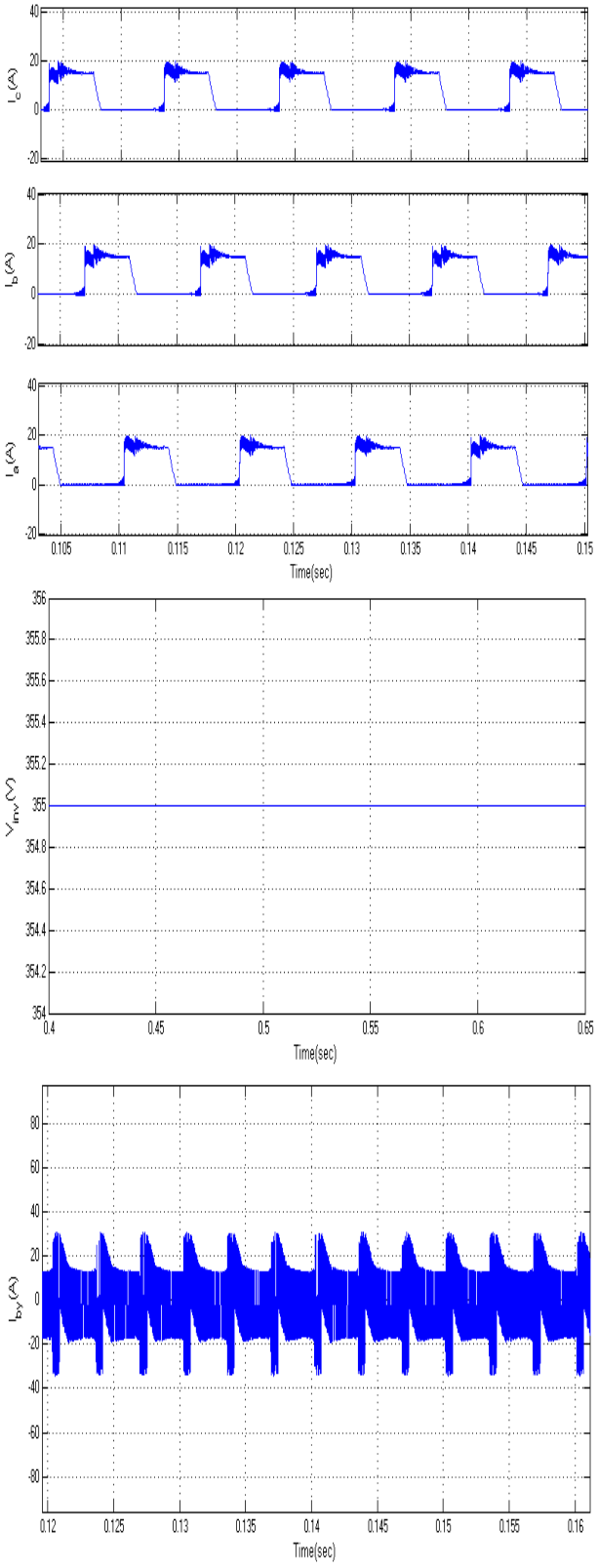

(a) Simulation results of driving-charging mode (mode 1)

International Journal For Advanced Research In Science & Technology
A peer reviewed international journal
www.ijarst.in
ISSN: 2457-0362

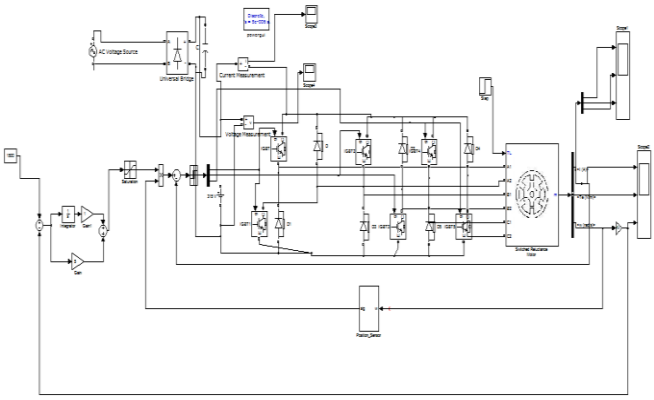

Fig.16 SRM drive model diagram

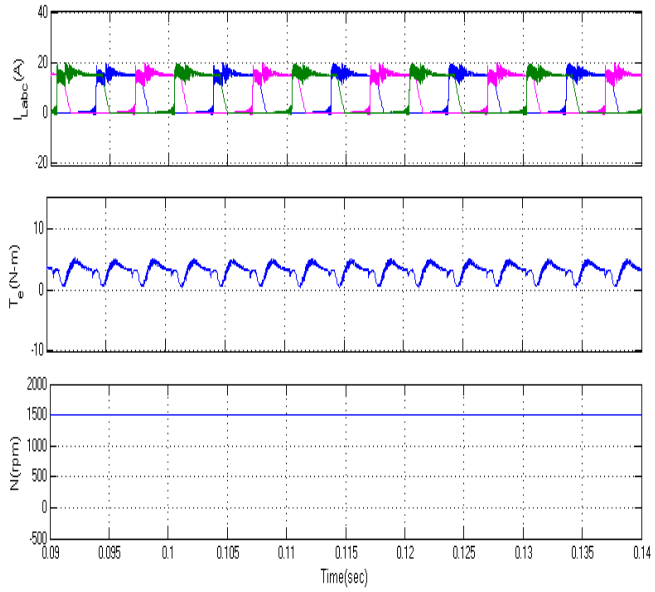

(b) Simulation results of single source driving mode (modes 3 and 4)

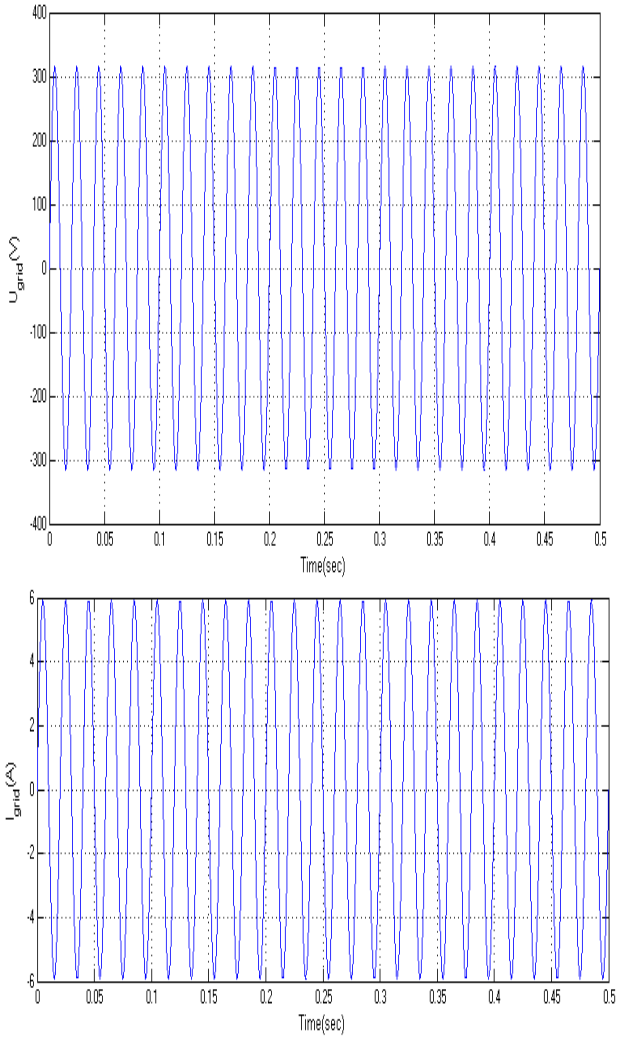

(a) Grid charging (mode 5)

Fig.17 Simulation results for driving conditions at modes 1, 3 and 4.

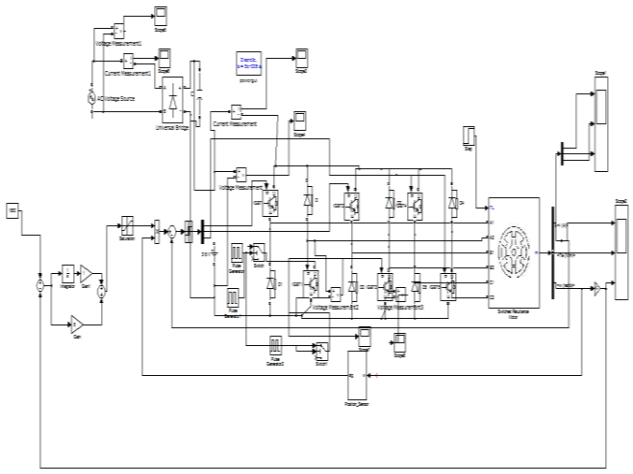

Fig.18 SRM drive model diagram

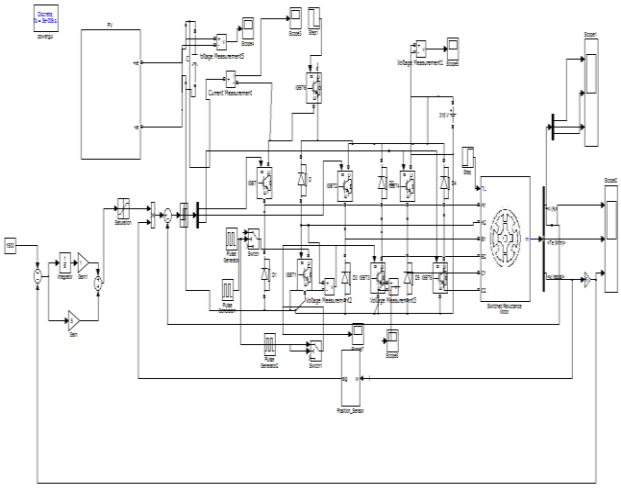

Fig.19 PV-powered SRM drive model diagram

International Journal For Advanced Research In Science & Technology
A peer reviewed international journal
www.ijarst.in
ISSN: 2457-0362

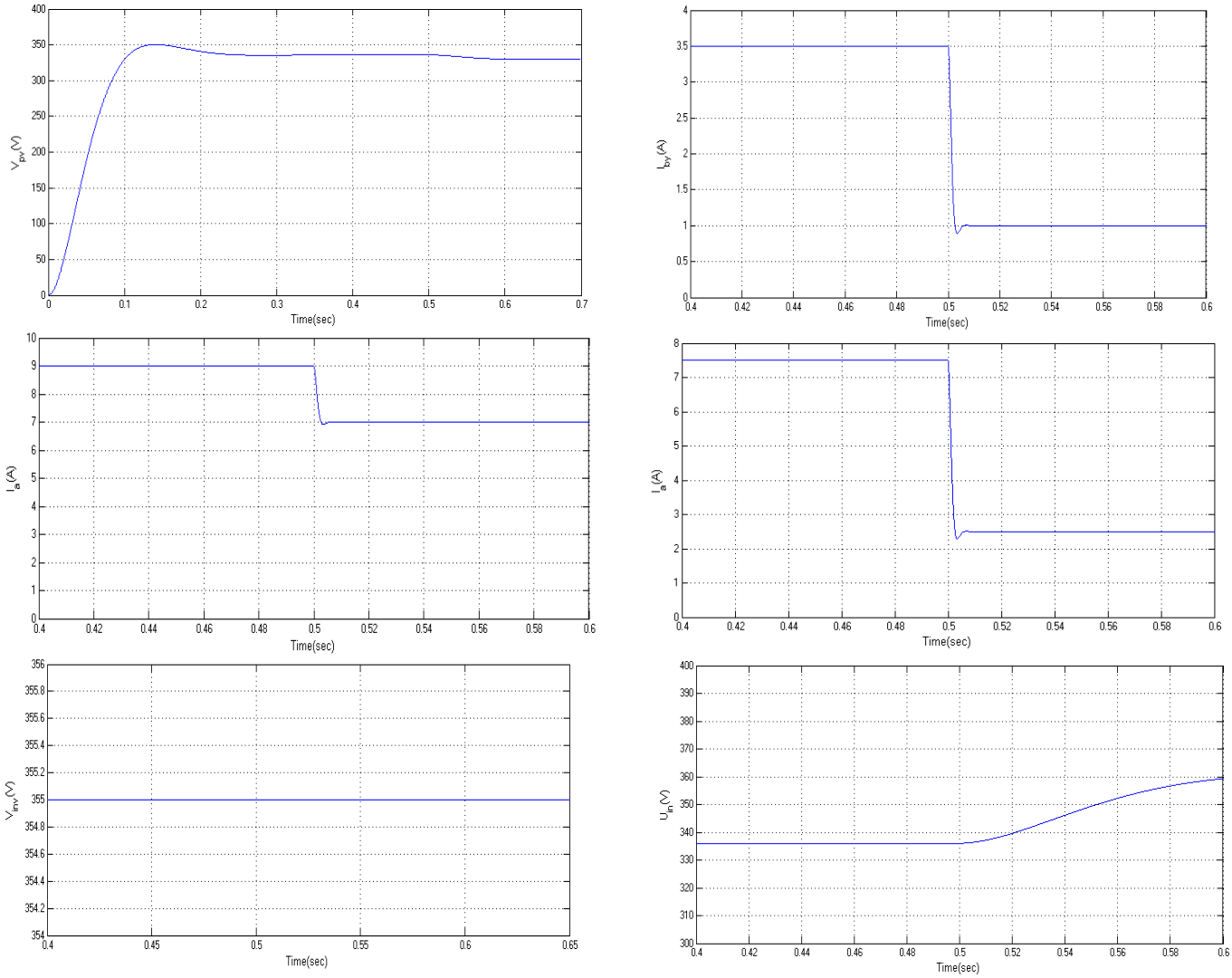

(b) PV charging mode 6 (stage 1 to stage 2)

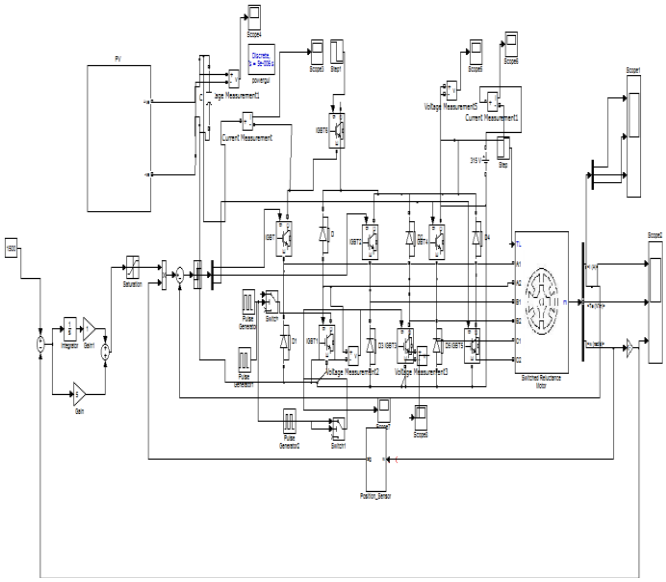

Fig.20 PV-powered SRM drive model diagram

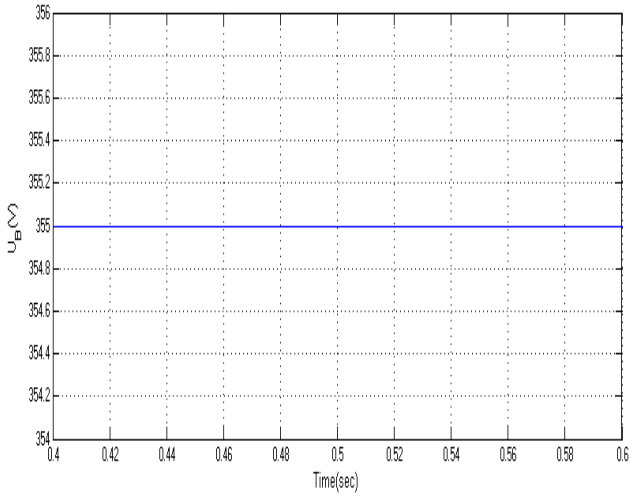

(c) PV charging mode 6 (stage 2 to stage 3)

Fig.21 simulation results for charging modes.

International Journal For Advanced Research In Science & Technology
A peer reviewed international journal
www.ijarst.in
ISSN: 2457-0362

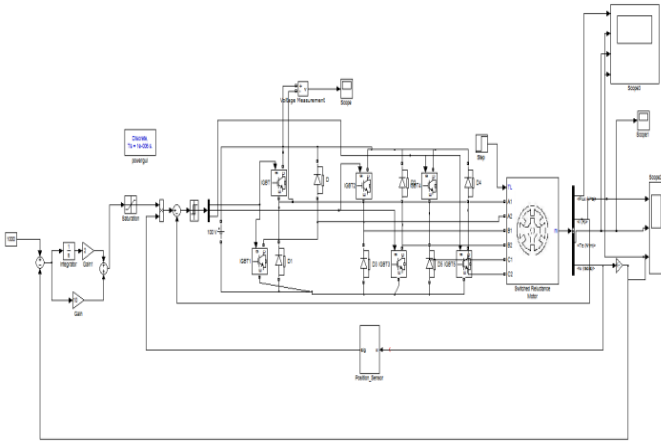

Fig.22 SRM drive model diagram With PI controller

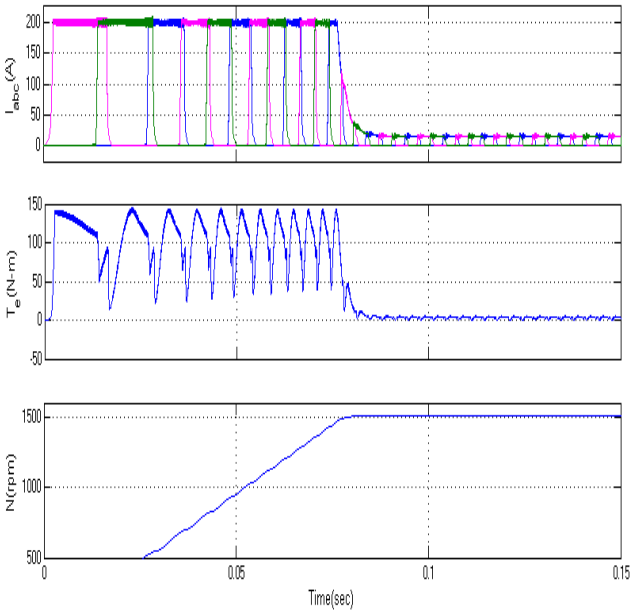

Fig.23 Flux, Current, Speed and Torque

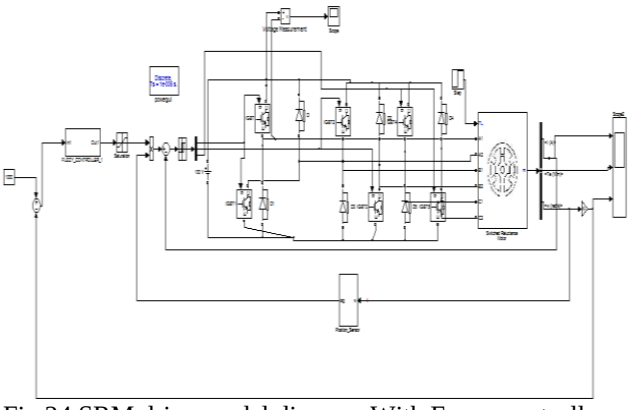

Fig.24 SRM drive model diagram With Fuzzy controller

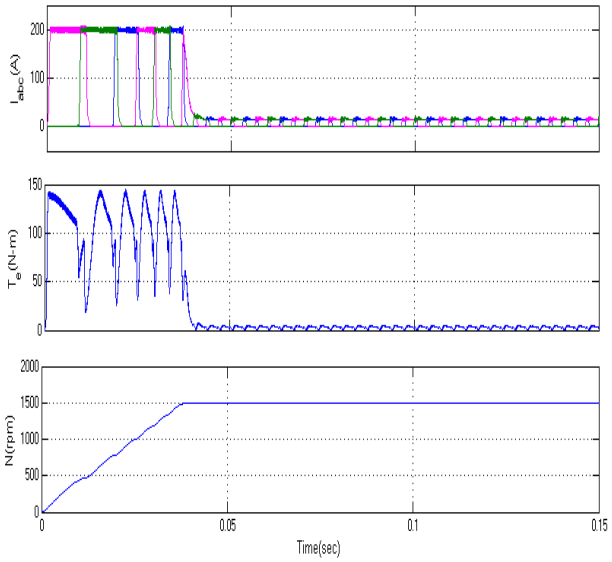

Fig.25 Current, Speed and Torque

VI. CONCLUSION

The dynamic performance of the SRM is implemented in this study using MATLAB/simulink. The speed control of the SRM motor is achieved by PI in traditional techniques. It is carried out using a Fuzzy Logic Controller in this case. The Fuzzy Logic Controller produces better output than the other controllers. The fuzzy logic controller ensures good reference tracking of switching reluctance motor drives in this suggested manner. This fuzzy logic controller improves speed regulation by providing the best speed tracking without overshoot.

REFERENCES

[1] A. Emadi, L. Young-Joo, K. Rajashekara, "Power electronics and motordrives in electric, hybrid electric, and plug-in hybrid electric vehicles,"IEEE Trans. Ind. Electron., vol. 55, no. 6, pp. 2237-2245, Jun. 2008.

[2] B. l. K. Bose, "Global energy scenario and impact of power electronics in21st century," IEEE Trans. Ind. Electron., vol. 60, no. 7, pp. 2638-2651,Jul. 2013.

[3] J. de Santiago, H. Bernhoff, B. Ekergård, S. Eriksson, S. Ferhatovic, R.Waters, and M. Leijon,"Electrical motor drivelines in commercial allelectric vehicles: a review," IEEE Trans. Veh. Technol., vol. 61, no. 2, pp.475-484, Feb. 2012.

[4] Z. Amjadi, S. S. Williamson, "Power-electronics-based solutions for plugin hybrid electric vehicle energy storage and management systems," IEEETrans. Ind. Electron., vol. 57, no. 2, pp. 608-616, Feb. 2010.

[5] A. Kuperman, U. Levy, J. Goren, A. Zafransky, and A. Savernin, "Batterycharger for electric vehicle traction battery switch station," IEEE Trans.Ind. Electron., vol. 60, no. 12, pp. 5391-5399, Dec. 2013.

[6] S. G. Li, S. M. Sharkh, F. C. Walsh, and C. N. Zhang, "Energy and batterymanagement of a plug-in series hybrid electric vehicle using fuzzy logic,"IEEE Trans. Veh. Technol., vol. 60, no. 8, pp. 3571-3585, Oct. 2011.
[7] C. H. Kim, M. Y. Kim, and G. W. Moon, "A modularized chargeequalizer using a battery monitoring IC for series-connected Li-Ion batteryStrings in electric vehicles," IEEE Trans. Power Electron., vol. 28, no. 8,pp. 3779-3787, May 2013.
[8] Z. Ping, Z. Jing, L.Ranran, T. Chengde, W. Qian, "Magneticcharacteristics investigation of an axial-axial flux compound-structurePMSM used for HEVs," IEEE Trans. Magnetics, vol. 46, no. 6, pp. 2191-2194, Jun. 2010.
[9] A. Kolli, O. Béthoux, A. De Bernardinis, E. Labouré, and G. Coquery,"Space-vector PWM control synthesis for an H-bridge drive in electricvehicles," IEEE Trans. Veh. Technol., vol.62, no.6, pp. 2441-2452, Jul.2013.
[10] S. M. Yang, and J. Y. Chen, "Controlled dynamic braking for switchedreluctance motor drives with a Ind. Electron., vol. 60, no. 9, pp. 5696- 5710, Oct. 2014.
rectifier front end," IEEE Trans. Ind.Electron., vol. 60, no. 11, pp. 4913- 4919, Nov. 2013.
[11] B. Bilgin, A. Emadi, M. Krishnamurthy, "Comprehensive evaluation ofthe dynamic performance of a 6/10 SRM for traction application inPHEVs," IEEE Trans. Ind. Electron., vol. 60, no. 7, pp. 2564-2575, July.2013.
[12] M. Takeno, A.Chiba, N. Hoshi, S. Ogasawara, M. Takemoto, M. A.Rahman, "Test results and torque improvement of the 50-kW switchedreluctance motor designed for hybrid electric vehicles," IEEE Trans. Ind.Appl., vol. 48, no. 4, pp. 1327-1334, Jul/Aug. 2012.
[13] A. Chiba, M. Takeno, N. Hoshi, M. Takemoto, S.Ogasawara, M. A.Rahman, "Consideration of number of series turns in switched-reluctancetraction motor competitive to HEV IPMSM," IEEE Trans. Ind. Appl., vol.48, no. 6, pp. 2333-2340, Nov/Dec. 2012.
[14] I. Boldea, L. N. Tutelea, L. Parsa, and D. Dorrell, "Automotive electricpropulsion systems with reduced or no permanent magnets: an overview,"IEEE Trans.